nature neuroscience

Local potassium signaling couples neuronal activity to vasodilation in the brain

Jessica A Filosa[1,2], Adrian D Bonev[1], Stephen V Straub[1], Andrea L Meredith[3,4], M Keith Wilkerson[1], Richard W Aldrich[3,4] & Mark T Nelson[1]

The mechanisms by which active neurons, via astrocytes, rapidly signal intracerebral arterioles to dilate remain obscure. Here we show that modest elevation of extracellular potassium (K^+) activated inward rectifier K^+ (Kir) channels and caused membrane potential hyperpolarization in smooth muscle cells (SMCs) of intracerebral arterioles and, in cortical brain slices, induced Kir-dependent vasodilation and suppression of SMC intracellular calcium (Ca^{2+}) oscillations. Neuronal activation induced a rapid (<2 s latency) vasodilation that was greatly reduced by Kir channel blockade and completely abrogated by concurrent cyclooxygenase inhibition. Astrocytic endfeet exhibited large-conductance, Ca^{2+}-sensitive K^+ (BK) channel currents that could be activated by neuronal stimulation. Blocking BK channels or ablating the gene encoding these channels prevented neuronally induced vasodilation and suppression of arteriolar SMC Ca^{2+}, without affecting the astrocytic Ca^{2+} elevation. These results support the concept of intercellular K^+ channel–to–K^+ channel signaling, through which neuronal activity in the form of an astrocytic Ca^{2+} signal is decoded by astrocytic BK channels, which locally release K^+ into the perivascular space to activate SMC Kir channels and cause vasodilation.

In the brain, increased neuronal activity is accompanied by an increase in local cerebral blood flow, which serves to satisfy enhanced glucose and oxygen demand. This linkage between neuronal activity and increased local blood flow—termed functional hyperemia—has been appreciated since the classic study of Roy and Sherrington[1] over 100 years ago, although the mechanisms by which increased synaptic activity is communicated to the cerebral microcirculation to generate a vasodilator response are poorly understood. However, recent studies have illuminated a central role for astrocytic Ca^{2+} signals as mediators of this process of neurovascular coupling[2–7]. Electrical stimulation of neurons or activation of astrocytic metabotropic glutamate receptors (mGluR) induces an astrocytic Ca^{2+} wave that propagates to astrocytic endfeet, which encase penetrating arterioles in the brain[2,7]. A proposed target of this Ca^{2+} signal in the endfoot is the Ca^{2+}-sensitive phospholipase A_2 (PLA_2), which is responsible for the production of arachidonic acid (AA). On the basis of the effects of cyclooxygenase (COX) blockers, it has been proposed that prostaglandin E_2 (PGE_2) mediates a significant component of the dilatory response[6,7]. The remaining Ca^{2+}-dependent, non–COX-dependent component has remained elusive[8]. Here, we test the hypothesis that BK channels, expressed in astrocytic endfeet[9], are sensors of astrocytic Ca^{2+} that signal to adjacent arteriolar SMCs through the local release of K^+ into the perivascular space.

Elevation of the concentration of external potassium ions ($[K^+]_o$) to levels sufficient to depolarize SMCs ($\geq$20 mM) induces vasoconstriction of cerebral arteries[10] and arterioles[11]. Paradoxically, a modest elevation of $[K^+]_o$ (<20 mM) is one of the most potent vasodilatory signals in the cerebrovasculature[10,12,13]. Elevation of $[K^+]_o$ activates strong inward rectifier K^+ channels[10,12], in particular the Kir2.1 channel, in SMCs isolated from cerebral arteries[14,15]. Increasing intravascular pressure from 10 mm Hg to 60 mm Hg depolarizes SMCs in cerebral (pial) arteries from about –63 mV to –45 mV, and elevation of $[K^+]_o$ to 16 mM results in Kir channel–mediated hyperpolarization of SMCs from –45 mV to about –58 mV, lowers average Ca^{2+} in SMCs in the arterial wall from 192 nM to 126 nM, and causes an approximately 60% vasodilation[10,16]. Although it is well established that extracellular cerebral (pial) arteries dilate to activation of SMC Kir channels, it is not known if these channels are expressed in SMCs of intracerebral (parenchymal) arterioles, and whether activation of these channels constitutes a mechanism through which active neurons induce vasodilation.

RESULTS

$[K^+]_o$ activation of Kir channels in arteriolar SMCs

To establish whether functional Kir channels are expressed in SMCs of parenchymal arterioles, we isolated single SMCs from these arterioles and measured K^+ currents using the whole-cell, perforated-patch-clamp technique. These currents exhibited characteristic properties of Kir2 channels: namely, steep activation with membrane potential

[1]Department of Pharmacology, 89 Beaumont Avenue, College of Medicine, University of Vermont, Burlington, Vermont 05405, USA. [2]Department of Psychiatry, University of Cincinnati, Cincinnati, Ohio 45237, USA. [3]Department of Molecular and Cellular Physiology and the Howard Hughes Medical Institute, Stanford University, Stanford, California 94305, USA. [4]Present addresses: Department of Physiology, University of Maryland School of Medicine, 655 West Baltimore Street (BRB5), Baltimore, Maryland 21201, USA (A.L.M.) and Section of Neurobiology, 1 University Station C7000, University of Texas at Austin, Austin, Texas 78712, USA (R.W.A.). Correspondence should be addressed to M.T.N. (Mark.Nelson@uvm.edu).

Received 28 April; accepted 6 September; published online 1 October 2006; doi:10.1038/nn1779

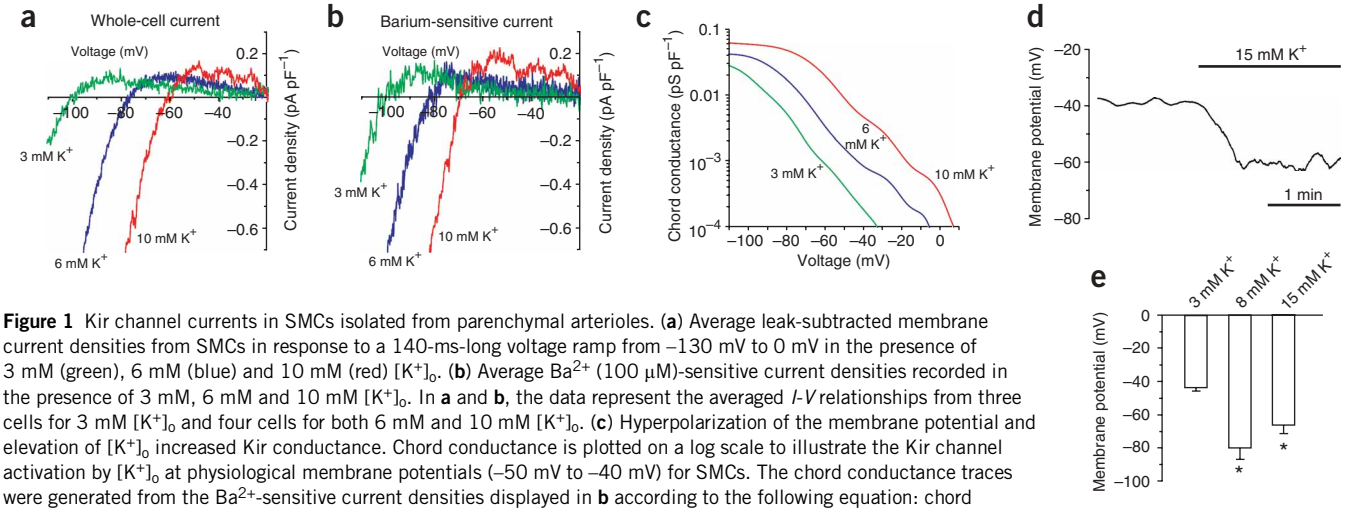

Figure 1 Kir channel currents in SMCs isolated from parenchymal arterioles. (**a**) Average leak-subtracted membrane current densities from SMCs in response to a 140-ms-long voltage ramp from –130 mV to 0 mV in the presence of 3 mM (green), 6 mM (blue) and 10 mM (red) $[K^+]_o$. (**b**) Average Ba^{2+} (100 μM)-sensitive current densities recorded in the presence of 3 mM, 6 mM and 10 mM $[K^+]_o$. In **a** and **b**, the data represent the averaged *I-V* relationships from three cells for 3 mM $[K^+]_o$ and four cells for both 6 mM and 10 mM $[K^+]_o$. (**c**) Hyperpolarization of the membrane potential and elevation of $[K^+]_o$ increased Kir conductance. Chord conductance is plotted on a log scale to illustrate the Kir channel activation by $[K^+]_o$ at physiological membrane potentials (–50 mV to –40 mV) for SMCs. The chord conductance traces were generated from the Ba^{2+}-sensitive current densities displayed in **b** according to the following equation: chord conductance = current density/($V - V_{rev}$), where V is the membrane potential and V_{rev} is the reversal potential for the current density. The current densities were first subjected to a fast Fourier transform (FFT) low-pass filter, which removes Fourier components with frequencies higher than 50 Hz. (**d**) Elevation of external $[K^+]_o$ from 3 mM to 15 mM caused a membrane potential hyperpolarization of SMCs in the wall of a pressurized (40 mm Hg) parenchymal arteriole from the cortex. (**e**) Summary data of the membrane potential of SMCs in pressurized (40 mm Hg) parenchymal arterioles in the presence of 3 mM, 8 mM and 15 mM $[K^+]_o$. Data represent mean ± s.e.m. The membrane potentials in 8 mM and 15 mM $[K^+]_o$ were significantly hyperpolarized relative to those in 3 mM $[K^+]_o$ (six arterioles, $P < 0.05$).

hyperpolarization, shift of the activation curve to more positive potentials with an elevation of $[K^+]_o$, potent inhibition by external barium (Ba^{2+}) ions, and strong rectification (**Fig. 1**). In fact, the current density of Kir currents at –100 mV (–16.4 pA pF^{-1} in 60 mM $[K^+]_o$) in arteriolar myocytes was greater than that in myocytes derived from pial arteries (–11.1 pA pF^{-1} in 60 mM $[K^+]_o$)[17]. Elevation of $[K^+]_o$ from 3 mM to 6 mM or 10 mM shifted the whole-cell and Ba^{2+}-sensitive (Kir) currents to more positive potentials (**Fig. 1a**,**b**) and increased Kir channel conductance at all membrane potentials (**Fig. 1c**). The half-activation voltage ($V_{0.5}$) of Kir channel conductance shifted with the K^+ equilibrium potential (E_K; ($V_{0.5}$ was –111.3 ± 0.1 mV in 3 mM $[K^+]_o$, –82.4 ± 0.1 mV in 6 mM $[K^+]_o$, and –68.0 ± 0.1 mV in 10 mM $[K^+]_o$; $n = 3$–4), and the equivalent gating charge was 2.5 ± 0.6, properties consistent with strong inward rectifier potassium channels[18]. Indeed, elevation of $[K^+]_o$ from 3 mM ($[K^+]_o$ in cerebrospinal fluid) to 10 mM increased the Kir current density 6.3-fold ($P < 0.05$) at –45 mV.

The relevant ionic currents that regulate the membrane potential of arterial SMCs are small (<1 pA; **Fig. 1** and refs. 18–20) and generally less than leak currents from the electrode seal (Methods). Furthermore, enzymatically isolated SMCs lose cell-cell coupling and are not subjected to constricting stimuli. Therefore, to determine the effect of $[K^+]_o$ on SMC membrane potential, we measured the membrane potential of SMCs in the wall of isolated intracerebral arterioles, using sharp microelectrodes. Parenchymal arterioles were pressurized to approximately physiological levels (40 mm Hg). Elevation of $[K^+]_o$ from 3 mM to 15 mM hyperpolarized the membrane potential of SMCs in isolated, pressurized parenchymal arterioles from about –40 mV to –60 mV (**Fig. 1d**), close to the estimated new E_K. This response would predict that elevation of $[K^+]_o$ to a level less than 15 mM might cause a greater hyperpolarization, as E_K would be more negative. Indeed, elevation of $[K^+]_o$ from 3 mM to 8 mM caused a membrane potential hyperpolarization from –44 ± 2 mV to –80 ± 7 mV (**Fig. 1e**), which is close to E_K (–76 mV) in 8 mM $[K^+]_o$.

Elevated $[K^+]_o$ potently dilates arterioles in brain

Given the relatively high Kir channel current density of arteriolar SMCs and the observation that $[K^+]_o$ induces hyperpolarization of SMCs in isolated parenchymal arterioles (**Fig. 1**), we predict that elevation of

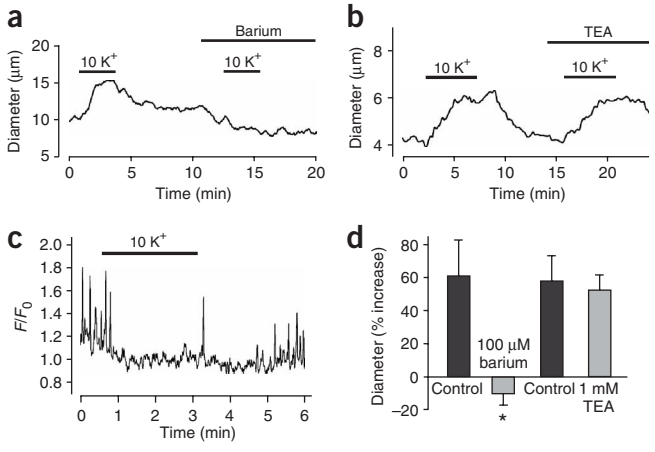

Figure 2 Elevation of $[K^+]_o$ to 10 mM dilates parenchymal arterioles and suppresses Ca^{2+} oscillations in arteriolar SMCs in brain slices. (**a**) Elevation of $[K^+]_o$ from 3 mM to 10 mM induced vasodilation of an arteriole within a cortical brain slice (**Supplementary Video 1**). This vasodilation was prevented by treatment with the Kir channel blocker Ba^{2+} (100 μM). (**b**) The BK channel blocker TEA (1 mM) did not prevent $[K^+]_o$ induced vasodilation of an arteriole within the slice. (**c**) Representative trace illustrating the reversible suppression of arteriolar SMC Ca^{2+} oscillations from a parenchymal arteriole exposed to 10 mM $[K^+]_o$. (**d**) Mean data (± s.e.m) illustrating that the Kir channel blocker Ba^{2+}, but not the BK channel blocker TEA, inhibits $[K^+]_o$-induced dilations of arterioles in brain slices ($n = 5$ each). In addition, treatment of arterioles with Ba^{2+} or TEA did not significantly alter arteriolar diameter. Mean diameter of arterioles in brain slices after ~15 min incubation in 100 μM Ba^{2+} was 96 ± 3% of control diameter ($n = 9$). Mean diameter of arterioles in brain slices after ~15 min incubation in 1 mM TEA was 100 ± 4% of control diameter ($n = 14$).

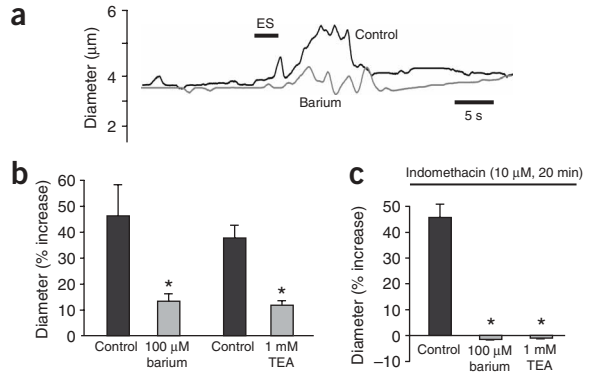

Figure 3 Neuronal activity–induced dilation of arterioles is largely inhibited by blockers of Kir or BK channels in brain slices. (**a**) Representative traces illustrating the inhibition of electrical stimulation–induced vasodilation of an arteriole in a cortical slice by Ba^{2+} (100 μM) (**Supplementary Videos 2** and **3**). (**b**) Mean data (± s.e.m) illustrating the block of electrical stimulation–induced vasodilation by Ba^{2+} and TEA ($n = 5$ each). (**c**) Mean data (± s.e.m) illustrating that Ba^{2+} and TEA completely block electrical stimulation–induced vasodilation in the presence of the COX inhibitor indomethacin ($n = 3$–4).

$[K^+]_o$ should dilate parenchymal arterioles in the brain. To evaluate the physiological response to $[K^+]_o$, we examined the effects of elevating $[K^+]_o$ to 10 mM on arteriolar diameter and SMC Ca^{2+} oscillations in brain slices, using infrared differential interference contrast (IR-DIC) imaging and fluorescence confocal microscopy, respectively. As is the case with other resistance arterioles, parenchymal arterioles *in vivo* are partially constricted because of intravascular pressure and other contractile stimuli. These arterioles often exhibit smooth muscle Ca^{2+} oscillations and vasomotion in brain slices[2], an observation that is supported by *in vivo* measurements[21,22]. To maintain arteriolar tone over the course of the experiments at a level observed in isolated, pressurized parenchymal arterioles, we applied low concentrations (100–150 nM) of the thromboxane A_2 receptor agonist (9,11-dideoxy-11α, 9α-epoxymethanoprostaglandin $F_{2\alpha}$ (U46619)) to cortical brain slices[23]. This approach permits the detection of processes that lead either to an increase or decrease of smooth muscle Ca^{2+} and arteriolar diameter.

Elevation of $[K^+]_o$ in the bath (artificial cerebrospinal fluid, aCSF) solution to 10 mM induced a reversible vasodilation (~60%) of parenchymal arterioles, and suppressed SMC Ca^{2+} oscillations, as measured by changes in fluo-4 fluorescence (**Fig. 2**, and **Supplementary Video 1** online). Ba^{2+} ions, which are relatively selective for Kir2 channels at low concentrations (<100 μM; ref. 17) blocked the $[K^+]_o$-induced vasodilation and suppression of SMC Ca^{2+} oscillations (percent inhibition of oscillation frequency = 68.7 ± 15.8% control versus 12.6 ± 6.0% in 100 μM Ba^{2+}). In fact, in the presence of Ba^{2+}, 10 mM $[K^+]_o$ constricted arterioles by an average of 9.8 ± 7.5% of resting diameter ($n = 5$; $P < 0.05$; **Fig. 2a**,**d**). Notably, 10 mM $[K^+]_o$ did not affect astrocytic endfoot Ca^{2+} (percent change in fractional fluorescence = 1.1 ± 2.3%; $n = 3$). In addition, tetraethylammonium ions (TEA, 1 mM), which act rapidly and are relatively selective for BK channels[24], did not alter the dilation to 10 mM $[K^+]_o$ (dilation = 58.2 ± 15.5% in control versus 52.6 ± 9.5% in TEA; $n = 5$; **Fig. 2b**,**d**), indicating that SMC BK channels are not directly involved in the arteriolar response to $[K^+]_o$. Furthermore, arteriolar diameter was not significantly altered by treatment with Ba^{2+} or TEA suggesting that, under these experimental conditions, neither Kir nor BK channels contribute substantially to the tone of parenchymal arterioles. These results support an important role for perivascular K^+ signaling through the activation of arteriolar SMC Kir channels in the dynamic regulation of cerebrovascular tone.

Neuronal activity induces Kir-dependent vasodilation

$[K^+]_o$ can act through smooth muscle Kir channels to lower SMC Ca^{2+} and induce dilation. However, the contribution of this mechanism to the rapid coupling between neuronal activity and vasodilation is not known. Using high spatial- and temporal-resolution confocal Ca^{2+} imaging of cortical brain slices, we previously determined that neuronal activity induced via field or focal electrical stimulation causes an elevation of astrocytic Ca^{2+} and a rapid suppression of SMC Ca^{2+} oscillations (ref. 2). Electrical stimulation for 3–5 s induced a 40–50% vasodilation of cerebral arterioles in brain slices with a latency (from the beginning of electrical stimulation to the onset of dilation) of 1.8 ± 0.4 s ($n = 10$; **Fig. 3a**). The rapid coupling of electrical stimulation and vasodilation is consistent with *in vivo* measurements of functional hyperemia[25,26]. Notably, this electrical stimulation–induced vasodilation was greatly reduced (~71%) by inhibition of Kir channels with 100 μM Ba^{2+} (46.3 ± 11.9% dilation in control versus 13.5 ± 2.6% dilation in Ba^{2+}, $n = 5$; $P < 0.05$; **Fig. 3a**,**b**). In time-matched control experiments in the absence of Ba^{2+} or TEA, the second electrical stimulation–induced vasodilation did not differ significantly from the first (vasodilation induced by the second electrical stimulation was 96 ± 5% of that induced by the first, $n = 11$; $P < 0.05$). Ba^{2+} did not affect electrical stimulation–induced astrocytic Ca^{2+} signals, consistent with fact that the locus of Ba^{2+} action is the arteriolar smooth muscle. These results support the hypothesis that SMC Kir channels are active participants in the process of neurovascular coupling.

On the basis of the effects of COX inhibition in neonatal rat brain slices, it has been suggested that an elevation of astrocytic Ca^{2+} leads to

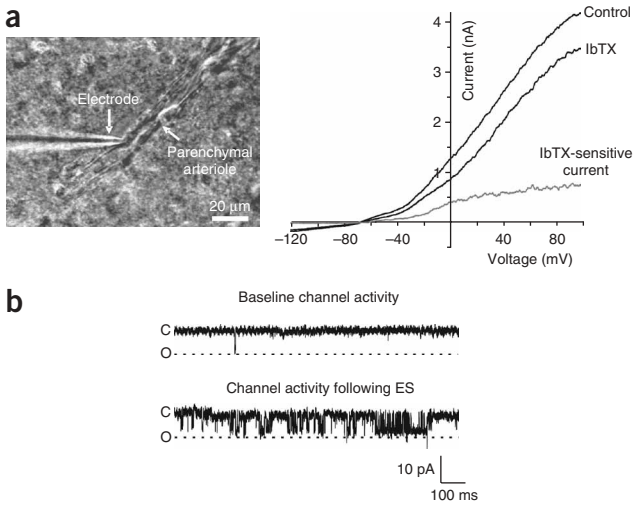

Figure 4 BK channel currents in astrocytic endfeet in brain slices. (**a**) *I-V* relationship of whole-cell astrocytic currents before and after 7 min exposure to the specific BK channel inhibitor IbTX (200 nM). Currents were recorded in response to 200-ms-long voltage ramps from –120 mV to 100 mV. Holding potential was –80 mV. The IbTX-sensitive (difference) current is shown in gray. Inset, positioning of the patch pipette on an endfoot in a brain slice. (**b**) Representative traces showing single BK channel currents in cell-attached patches from an astrocytic endfoot before (upper trace) and immediately after (lower trace) electrical stimulation (ES). C, closed; O, open. Holding potential was 0 mV. The $[K^+]_o$ was 6 mM in these experiments.

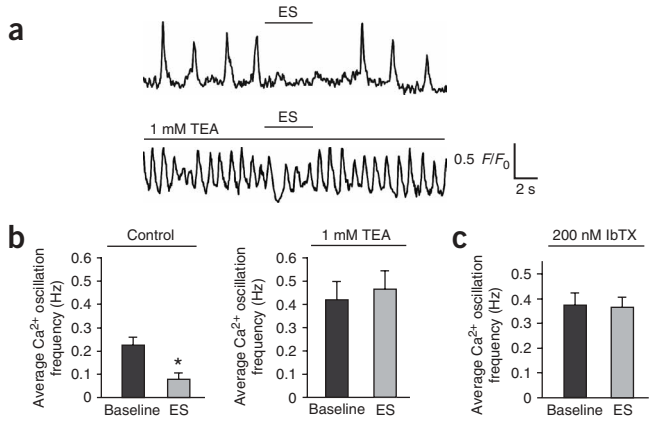

Figure 5 Blockade of BK channels inhibits electrical stimulation–induced suppression of arteriolar smooth muscle Ca^{2+} oscillations in brain slices. (**a**) Representative traces illustrating the suppression of smooth muscle arteriolar Ca^{2+} oscillations after electrical stimulation (upper trace), and inhibition of the electrical stimulation–induced suppression of arteriolar Ca^{2+} oscillations in the presence of the BK channel blocker TEA (1 mM) (lower trace). (**b**) Electrical stimulation reduced mean (± s.e.m) arteriolar Ca^{2+} oscillation frequency (Hz) in control by approximately 65% (left), but had no effect in the presence of TEA (right). $n = 11$–12. TEA elevated the mean frequency about twofold. (**c**) Electrical stimulation did not affect mean (± s.e.m) arteriolar Ca^{2+} oscillations in slices preincubated for 20 min with the specific BK channel blocker IbTX (200 nM, $n = 12$). Inhibition of SMC Ca^{2+} oscillation frequency was reproducible over multiple electrical stimulations (inhibition due to first electrical stimulation was 58.7 ± 6.9%; that due to second stimulation was 62.8 ± 6.7; $n = 10$). The $[K^+]_o$ was 6 mM in these experiments.

the generation of a COX product, namely PGE_2, which contributes to vasodilation presumably through activation of vascular SMC prostaglandin receptors[7]. More recently, *in vivo* studies demonstrated that the release of caged Ca^{2+} in endfeet causes a rapid vasodilation that is attenuated by COX inhibition[6]. To elucidate the role of Kir channels in the absence of COX activity, we examined the effects of channel blockers in the presence of the COX inhibitor indomethacin (10 μM, 20–25 min incubation). In the presence of indomethacin, electrical stimulation still caused a significant vasodilation (45.8 ± 5.2% increase in diameter; $n = 4$; **Fig. 3c**) that was completely inhibited by the subsequent addition of the Kir channel blocker Ba^{2+} (100 μM; –1.5 ± 0.1% diameter change; $n = 4$; $P < 0.05$), suggesting that the role of Kir channels is independent of COX activity.

Involvement of astrocytic BK channels

Astrocytic processes envelope parenchymal arterioles and are in close apposition to the arteriolar SMC membrane[27,28]. Because astrocytic Ca^{2+} signals seem to have a central role in communicating neuronal activity to arterioles[2,5–7,29] and external K^+ is a potent dilator of parenchymal arterioles, we tested the hypothesis that Ca^{2+}-sensitive BK channels in astrocytic endfeet act as transducers of the neuronally derived information encoded in the astrocytic Ca^{2+} signal.

BK channels are uniquely suited to deliver high local K^+ concentrations by virtue of their Ca^{2+} sensitivity and the high flux of K^+ ions through the open channel, even with a small driving force. Based on immunocytochemistry, BK channels appear to be clustered in astrocytic endfeet[9]. Furthermore, the close proximity of astrocytic endfoot BK channels to parenchymal smooth muscle suggests that only a small increase in BK channel activity would be required to release sufficient K^+ into the perivascular space to cause vasodilation. Indeed, the opening of a single BK channel for 0.2 s should be sufficient to provide enough K^+ ions (about 10^6) in the restricted space between astrocytic endfeet and SMCs to elevate the local K^+ concentration to 10 mM (using the unitary current measured at resting potential, and assuming that the distance from the endfoot to smooth muscle is 20 nm (ref. 27) and that the endfoot surface area is about 80 μm^2 (ref. 30)).

Astrocytes exhibit a characteristic high K^+ conductance[31]. Although BK channels are preferentially expressed in astrocytic endfeet[9] and functional BK channels have been demonstrated in cultured astrocytes[32], BK currents have not been previously measured in the endfeet of native astrocytes in brain slices. We therefore examined the contribution of BK channels to astrocytic K^+ currents, using the perforated-patch configuration of the whole-cell patch-clamp technique on astrocytic endfeet. On the basis of the effects of the specific BK channel blocker iberiotoxin (IbTX, 200 nM), we found that at least 38.1 ± 7.7% ($n = 5$) of the K^+ current at 0 mV was carried by BK channels (**Fig. 4a**). To determine the effect of neuronal activation on BK channels, we measured single-channel currents from astrocytic endfeet using the on-cell configuration. Electrical stimulation increased the open probability (NPo) of single channels on astrocytic endfeet 160 ± 71 times ($n = 4$), with a unitary conductance (slope conductance, 225.6 ± 20.0 pS, $n = 3$ endfeet) consistent with that previously determined for BK channels

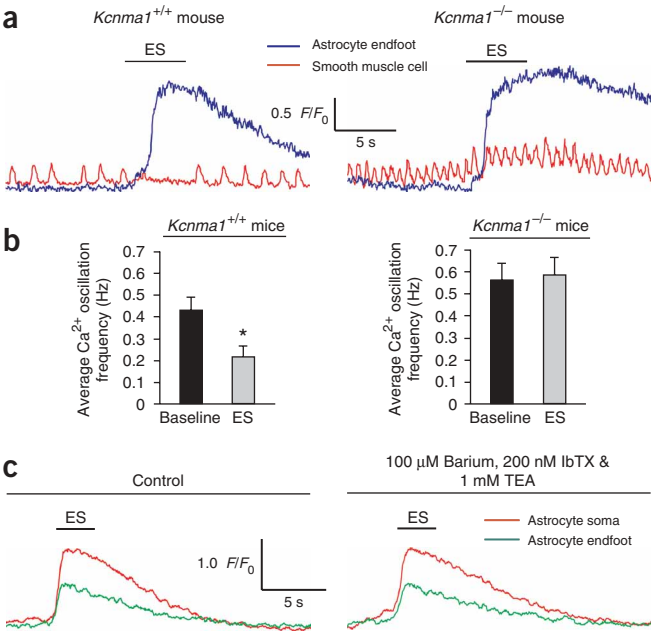

Figure 6 The absence of functional BK channels prevents electrical stimulation–induced suppression of Ca^{2+} oscillations in SMCs of parenchymal arterioles in brain slices. (**a**) Representative recordings illustrating simultaneous Ca^{2+} changes in an astrocytic endfoot (blue) and a vascular SMC (red) in cortical brain slices from *Kcnma1*$^{+/+}$ (left) and *Kcnma1*$^{-/-}$ (right) mice. Electrical stimulation induced a rise in astrocytic Ca^{2+} in brain slices from both types of mice, and suppressed smooth muscle Ca^{2+} oscillations in *Kcnma1*$^{+/+}$, but not *Kcnma1*$^{-/-}$, mice. (**b**) Mean (± s.e.m) arteriolar Ca^{2+} oscillation frequency (Hz) before and during electrical stimulation from *Kcnma1*$^{+/+}$ mice ($n = 17$) and *Kcnma1*$^{-/-}$ ($n = 12$) mice. Electrical stimulation reduced arteriolar Ca^{2+} oscillations frequency by 50% in *Kcnma1*$^{+/+}$, but had no effect in *Kcnma1*$^{-/-}$ mice. (**c**) Astrocytic Ca^{2+} transients from a rat brain slice following electrical stimulation in the absence (left) and the presence (right) of the Kir and BK channel blockers $BaCl_2$, IbTX and TEA. The $[K^+]_o$ was 6 mM in these experiments.

(**Fig. 4b**). Collectively, these results support the concept that neuronal stimulation induces an elevation of intracellular Ca^{2+} and activates BK channels in astrocytic endfeet, leading to the release of K^+ ions into the restricted space between the endfeet and the adjacent SMCs of the arterioles (**Supplementary Figure 1** online).

To determine whether astrocytic BK channels are involved in neurovascular coupling, we tested the effects of the BK channel inhibitor TEA on electrical stimulation–induced vasodilation and suppression of arteriolar Ca^{2+} oscillations in rat cortical brain slices. TEA reduced electrical stimulation–induced vasodilation by 69% (37.8 ± 5.0% dilation control versus 11.9 ± 1.6% dilation in TEA; $n = 5$; $P < 0.05$; **Fig. 3b**), and completely prevented vasodilation in the presence of indomethacin (–1.0 ± 0.1% diameter change; $n = 3$; $P < 0.05$; **Fig. 3c**). In the presence of the BK channel blockers TEA or IbTX (200 nM), electrical stimulation also failed to suppress Ca^{2+} oscillations in the SMCs of the arterioles (Ca^{2+} oscillation frequency in TEA: 0.42 ± 0.08 Hz baseline versus 0.47 ± 0.08 Hz following electrical stimulation, $n = 11$; in IbTX: 0.38 ± 0.05 Hz baseline versus 0.37 ± 0.03 Hz following electrical stimulation, $n = 12$; **Fig. 5**). These results indicate that functional BK channels are required for this mode of rapid neurovascular coupling. Furthermore, the observation that TEA had an inhibitory effect on electrical stimulation–induced vasodilation that is comparable (70% reduction) to that of the Kir channel blocker Ba^{2+} (compare **Fig. 3b**,**c**) provides further evidence that these two channels act in series.

To provide additional evidence for the role of BK channels in neurovascular coupling, we used brain slices from mice lacking the gene for the pore-forming alpha subunit of the BK channel (that is, *Kcnma1*$^{-/-}$ mice). These mice exhibit a number of pathologies including ataxia, an overactive bladder and incontinence[33]. Parenchymal arterioles in brain slices from both *Kcnma1*$^{+/+}$ and *Kcnma1*$^{-/-}$ mice exhibited smooth muscle Ca^{2+} oscillations and vasomotion. As expected, electrical stimulation significantly suppressed arteriolar smooth muscle Ca^{2+} oscillations in *Kcnma1*$^{+/+}$ mice (Ca^{2+} oscillation frequency = 0.44 ± 0.05 Hz in control versus 0.22 ± 0.05 Hz following electrical stimulation; $n = 17$; $P < 0.05$; **Fig. 6a**,**b**). In contrast, arteriolar smooth muscle Ca^{2+} oscillations in brain slices from *Kcnma1*$^{-/-}$ mice were unaffected by neuronal stimulation (0.57 ± 0.07 Hz control versus 0.59 ± 0.08 Hz following electrical stimulation; $n = 12$; **Fig. 6a**,**b**). This failure of astrocyte–to–smooth muscle communication in *Kcnma1*$^{-/-}$ mice could not be attributed to a disruption of neuron-to-astrocyte communication, as the electrical stimulation–induced astrocytic Ca^{2+} elevation was maintained (**Fig. 6a**). Electrical stimulation–induced astrocytic Ca^{2+} elevations were similarly unaffected by simultaneous block of BK and Kir channels in rat cortical brain slices (**Fig. 6c**). Electrical stimulation–induced increases in peak astrocytic Ca^{2+}, as measured by changes in fractional fluorescence, were 3.97 ± 0.68 in the astrocytic soma and 2.80 ± 0.30 in endfeet under control conditions, and 3.57 ± 0.26 in the soma and 2.63 ± 0.14 in endfeet in the presence of 200 nM IbTX, 100 μM $BaCl_2$ and 1 mM TEA ($n = 3$; **Fig. 6c**). These results strongly suggest that the activation of BK channels involved in mediating neuron-to-arteriole communication occurs downstream of the astrocytic Ca^{2+} elevation induced by neuronal stimulation.

DISCUSSION

It has long been proposed, based largely on studies of Müller cells in the retina, that the K^+ ions released from active neurons are 'siphoned' to regions of lower K^+ near the microvasculature[34,35]. Our results suggest an alternative concept for cortical astrocytes. (i) Information from active neurons is integrated by astrocytes, which generate increases in endfoot Ca^{2+} as a result of glutamate receptor activation and inositol 1,4,5-trisphosphate production. (ii) This elevation of endfoot Ca^{2+} activates BK channels, which release K^+ ions into the restricted space between the endfoot and the SMCs of the arteriole. (iii) The local elevation of external K^+ activates SMC Kir channels, thus causing SMC membrane potential hyperpolarization, which closes voltage-dependent Ca^{2+} channels, decreases intracellular Ca^{2+} and leads to vasodilation (**Supplementary Fig. 1**).

This mechanism assigns an important physiological role to the well-characterized responsiveness of the cerebrovascular circulation to elevation of $[K^+]_o$, and provides for fine and rapid regulation of arterial diameter. In addition, it could explain apparently paradoxical and opposing effects of astrocyte activation on arterial diameter[2,5–7], as the response of arterioles would depend on the amount of K^+ released from the astrocytic endfeet. Accordingly, higher concentrations of K^+ ($\geq$20 mM) released from the astrocytic endfeet through BK channels could lead to vasoconstriction through depolarization of arterial smooth muscle, whereas lower concentrations of astrocytic endfeet K^+ release ($<$20 mM) would cause membrane hyperpolarization of arteriolar smooth muscle and vasodilation. Furthermore, activation of any hyperpolarizing process (for example, electrogenic sodium or potassium ATPase or K_{ATP} channels[36]) in SMCs would also lead to an engagement of Kir channels through their steep voltage dependence.

The proposed model depicts a new mode of intercellular communication that relies on K^+ channel–to–K^+ channel signaling. The localized release of K^+ by endfoot BK channels and the spatial proximity of smooth muscle Kir channel targets are reminiscent of Ca^{2+} spark activation of closely apposed BK channels in smooth muscle[37]. As with Ca^{2+} spark activation of smooth muscle BK channels, astrocyte-derived, BK channel–mediated 'K^+ sparks' could serve to promote vasodilation through the activation of juxtaposed arteriolar smooth muscle Kir channels (**Supplementary Fig. 1**).

Notably, this is the first study to identify a specific vascular target involved in neurovascular coupling. Our findings suggest that alterations in smooth muscle Kir channel or astrocytic BK channel function could contribute to cerebrovascular disorders involving local cerebral ischemia[38,39] (that is, dementia and Alzheimer disease) and may explain the neuroprotective effects of BK channel openers[40–43].

METHODS

Brain slice preparation. Cortical brain slices were prepared from juvenile ($>$20 d old) Sprague-Dawley rats and from adult *Kcnma1*$^{+/+}$ and *Kcnma1*$^{-/-}$ mice, following protocols approved by the Office of Animal Care Management at the University of Vermont. The cortex was rapidly removed, cut into ~200-μm-thick coronal slices using a vibratome (Leica VT 1000S) in cold aCSF containing 3mM KCl, 125 mM NaCl, 1 mM $MgCl_2$, 26 mM $NaHCO_3$, 1.25 mM NaH_2PO_4, 10 mM glucose, 2 mM $CaCl_2$ and 400 μM L-ascorbic acid, equilibrated with 95% O_2 and 5% CO_2. Ascorbic acid was added to reduce cell swelling associated with oxidative stress. In experiments presented in **Figures 4–6**, KCl and NaCl concentrations were 6 mM and 122 mM, respectively, to allow direct comparison with previously published data[2,10,16]. Slices were immediately incubated at room temperature (21–24 °C) in aCSF equilibrated with 95%O_2 and 5%CO_2 (pH ≈ 7.45) until needed.

Ca^{2+} imaging. Ca^{2+} imaging was performed using a Solamere confocal unit (QLC 100) in combination with a high-sensitivity and high-resolution camera (XR MEGA-10, Stanford Photonics). Cortical slices were incubated at room temperature in aCSF containing 10 μM Fluo-4 AM and pluronic acid (2.5 μg ml^{-1}, Molecular Probes). After a 2- to 3-h incubation period, slices were washed and placed in aCSF until needed. At the time of the experiment, a slice was transferred to a perfusion chamber and continuously superfused with aCSF maintained at 35–37 °C. Parenchymal arterioles and astrocytes were visualized

with a 60× water-dipping objective (NA 1.0). Fluorescence images were obtained using a krypton/argon laser at 488 nm, and emitted light was captured at >495 nm. Images were acquired at 30 or 60 frames per s for ~60 s.

Video imaging. Video microscopy was used to determine arteriolar diameter changes, using IR-DIC and a CCD camera (Hamamatsu). Images were acquired at 30 images per s and stored for later analysis. Internal diameter changes were determined from the distance between multiple points across the arteriolar lumen. The internal diameter of arterioles investigated in this study was between ~4–20 μm, consistent with other studies of arterioles in cortical brain slices[44].

Electrical stimulation. Neuronal stimulation was performed by applying a 50-Hz alternating square pulse of 0.3 ms duration for 3–5 s using either a pair of platinum wires placed parallel to the brain slice or a pair of concentric bipolar electrodes placed several micrometers away from the vessel wall and, if possible, in the vicinity of a nearby astrocyte. The voltage required for electrical stimulation varied with the distance between the electrodes and the cellular targets. Electrical stimulation–induced effects are known to be blocked by the inhibition of voltage-dependent sodium channels by tetrodotoxin, indicating neuronal activation[2,7].

Isolation of single myocytes from parenchymal arterioles. Parenchymal arterioles were carefully dissected from the cerebral cortex and then digested with papain (0.3 mg ml^{-1} and 1 mg ml^{-1} dithioerythritol for 12 min at 37 °C) and collagenase (1 mg ml^{-1} collagenase, type F and type H in a 70%/30% mixture, incubated for 5 min at 37 °C). The digested tissue was gently triturated with fire-polished glass Pasteur pipettes to yield single myocytes. The mean cell capacitance was 9.2 ± 0.7 pF ($n = 16$).

Electrophysiological recordings. Whole-cell (perforated-patch configuration) and single-channel currents were amplified by an Axopatch 200B and analyzed using Clampfit 9.2 software (Axon Instruments). Whole-cell currents were filtered at 1 kHz and digitized at 10 kHz. Single-channel currents were filtered at 2 kHz and digitized at 10 kHz. Open probability was determined using the half-crossing method. Pipette solution for whole-cell configuration (perforated patch) consisted of 30 mM KCl, 110 mM potassium aspartate, 10 mM NaCl, 1 mM $MgCl_2$, 10 mM HEPES (adjusted to pH 7.2 with NaOH) and 250 μg ml^{-1} amphotericin B. Pipette solution for on-cell single-channel recordings consisted of 150 mM KCl, 1 mM $MgCl_2$ and 10 mM HEPES (adjusted to pH 7.2 with KOH). For whole-cell and single-channel recordings from astrocyte endfeet, brain slices were continuously superfused with aCSF at 35–37 °C. The bathing solution for whole-cell recordings from isolated arteriole myocytes consisted of 6 mM KCl, 134 mM NaCl, 2 mM $CaCl_2$, 1 mM $MgCl_2$, 10 mM HEPES and 10 mM glucose (adjusted to pH 7.4 with NaOH), and was maintained at room temperature. KCl concentration was changed to 3 mM, 10 mM or 60 mM by substituting NaCl for KCl. Whole-cell seal resistances varied from 10 GΩ to 20 GΩ, corresponding to –10 pA to –5 pA of leak current at –100 mV. Therefore, the leak current was larger than relevant physiological currents (for example, see **Fig. 1b**). Voltage-dependent K^+ channel activity, other than Kir channels, is minimal negative to –60 mV. Therefore, Ba^{2+}-insensitive currents between –60 mV and –80 mV were considered leak currents and were extrapolated over the entire voltage range in order to subtract leak currents from the whole-cell current. The magnitude of the subtracted leak current ranged from –1.5 pA to –6.2 pA (–3.6 ± 0.6 pA average; $n = 11$) at –60 mV. This linear leak current was subtracted from the whole-cell currents to obtain the data depicted in **Figure 1a**.

Arteriolar membrane potential recording. Brains were removed into MOPS-buffered saline containing 145 mM NaCl, 3 mM KCl, 1.2 mM NaH_2PO_4, 1.17 mM $MgSO_4$, 2.0 mM $CaCl_2$, 5 mM glucose, 0.02 mM EDTA, 3 mM MOPS and 10 mg ml^{-1} bovine serum albumin (pH 7.4) at 4 °C. Middle cerebral arteries with attached, penetrating parenchymal arterioles were carefully dissected from the brain, and parenchymal arterioles (30–40 μm diameter) were isolated from middle cerebral arteries and cannulated to resistance-matched micropipettes. Vessels were pressurized to 40 mm Hg and monitored throughout the experiment. Microelectrodes were filled with 500 mM KCl to produce electrode resistances of 100–200 MΩ, and potential was measured using a WPI Intra 767 amplifier.

Data analysis. Ca^{2+} imaging and arteriolar diameter experiments were analyzed with custom software created by A. Bonev. Fractional fluorescence (F/F_0) was determined by dividing the fluorescence intensity (F) within a region of interest (ROI) by a baseline fluorescence value (F_0) determined from ~50 images showing no activity. The frequency of Ca^{2+} oscillations was determined within an ROI (10 × 10 square pixels, or 2.5 × 2.5 μm^2) on a cell exhibiting Ca^{2+} oscillations. The number of peaks over a given time was automatically detected from oscillations crossing a set threshold value (>1.15 F/F_0). Data are expressed as mean ± s.e.m. Differences between two means were determined using Student's t-test. Statistical significance was tested at 95% ($P < 0.05$) confidence level.

Drugs. Thromboxane agonist U46619 was obtained from Sigma or Calbiochem, and IbTX was obtained from Peptides International. TEA, $BaCl_2$ and all other chemicals were obtained from Sigma.

Note: Supplementary information is available on the Nature Neuroscience website.

ACKNOWLEDGMENTS

We thank D. Hill-Eubanks for comments on the manuscript and J. Brayden for help with the microelectrode recordings. This work was supported by the US National Institutes of Health (grants HL44455 and HL63722 to M.T.N. from the National Heart, Lung and Blood Institute), a postdoctoral fellowship from the American Heart Association (0425923T to J.A.F.), a National Institutes of Health training grant (HL07944 to M.K.W.), the Howard Hughes Medical Institute and the Totman Trust for Medical Research.

COMPETING INTERESTS STATEMENT

The authors declare that they have no competing financial interests.

Published online at http://www.nature.com/natureneuroscience
Reprints and permissions information is available online at http://npg.nature.com/reprintsandpermissions/

1. Roy, C.S. & Sherrington, C. On the regulation of the blood supply of the brain. *J. Physiol. (Lond.)* **11**, 85–108 (1890).
2. Filosa, J.A., Bonev, A.D. & Nelson, M.T. Calcium dynamics in cortical astrocytes and arterioles during neurovascular coupling. *Circ. Res.* **95**, e73–e81 (2004).
3. Chaigneau, E., Oheim, M., Audinat, E. & Charpak, S. Two-photon imaging of capillary blood flow in olfactory bulb glomeruli. *Proc. Natl. Acad. Sci. USA* **100**, 13081–13086 (2003).
4. Metea, M.R. & Newman, E.A. Glial cells dilate and constrict blood vessels: a mechanism of neurovascular coupling. *J. Neurosci.* **26**, 2862–2870 (2006).
5. Mulligan, S.J. & MacVicar, B.A. Calcium transients in astrocyte endfeet cause cerebrovascular constrictions. *Nature* **431**, 195–199 (2004).
6. Takano, T. *et al.* Astrocyte-mediated control of cerebral blood flow. *Nat. Neurosci.* **9**, 260–267 (2006).
7. Zonta, M. *et al.* Neuron-to-astrocyte signaling is central to the dynamic control of brain microcirculation. *Nat. Neurosci.* **6**, 43–50 (2003).
8. Rossi, D.J. Another BOLD role for astrocytes: coupling blood flow to neural activity. *Nat. Neurosci.* **9**, 159–161 (2006).
9. Price, D.L., Ludwig, J.W., Mi, H., Schwarz, T.L. & Ellisman, M.H. Distribution of rSlo Ca^{2+}-activated K^+ channels in rat astrocyte perivascular endfeet. *Brain Res.* **956**, 183–193 (2002).
10. Knot, H.J., Zimmermann, P.A. & Nelson, M.T. Extracellular K(+)-induced hyperpolarizations and dilatations of rat coronary and cerebral arteries involve inward rectifier K(+) channels. *J. Physiol. (Lond.)* **492**, 419–430 (1996).
11. Horiuchi, T., Dietrich, H.H., Hongo, K. & Dacey, R.G., Jr. Mechanism of extracellular K^+-induced local and conducted responses in cerebral penetrating arterioles. *Stroke* **33**, 2692–2699 (2002).
12. McCarron, J.G. & Halpern, W. Potassium dilates rat cerebral arteries by two independent mechanisms. *Am. J. Physiol.* **259**, H902–H908 (1990).
13. Kuschinsky, W., Wahl, M., Bosse, O. & Thurau, K. Perivascular potassium and pH as determinants of local pial arterial diameter in cats. A microapplication study. *Circ. Res.* **31**, 240–247 (1972).
14. Zaritsky, J.J., Eckman, D.M., Wellman, G.C., Nelson, M.T. & Schwarz, T.L. Targeted disruption of Kir2.1 and Kir2.2 genes reveals the essential role of the inwardly rectifying K(+) current in K(+)-mediated vasodilation. *Circ. Res.* **87**, 160–166 (2000).
15. Bradley, K.K. *et al.* Kir2.1 encodes the inward rectifier potassium channel in rat arterial smooth muscle cells. *J. Physiol. (Lond.)* **515**, 639–651 (1999).
16. Knot, H.J. & Nelson, M.T. Regulation of arterial diameter and wall [Ca^{2+}] in cerebral arteries of rat by membrane potential and intravascular pressure. *J. Physiol. (Lond.)* **508**, 199–209 (1998).
17. Quayle, J.M., McCarron, J.G., Brayden, J.E. & Nelson, M.T. Inward rectifier K^+ currents in smooth muscle cells from rat resistance-sized cerebral arteries. *Am. J. Physiol.* **265**, C1363–C1370 (1993).
18. Quayle, J.M., Nelson, M.T. & Standen, N.B. ATP-sensitive and inwardly rectifying potassium channels in smooth muscle. *Physiol. Rev.* **77**, 1165–1232 (1997).

19. Nelson, M.T., Patlak, J.B., Worley, J.F. & Standen, N.B. Calcium channels, potassium channels, and voltage dependence of arterial smooth muscle tone. *Am. J. Physiol.* **259**, C3–18 (1990).
20. Nelson, M.T. & Quayle, J.M. Physiological roles and properties of potassium channels in arterial smooth muscle. *Am. J. Physiol.* **268**, C799–C822 (1995).
21. Mayhew, J.E. *et al.* Cerebral vasomotion: a 0.1-Hz oscillation in reflected light imaging of neural activity. *Neuroimage* **4**, 183–193 (1996).
22. Nilsson, H. & Aalkjaer, C. Vasomotion: mechanisms and physiological importance. *Mol. Interv.* **3**, 79–89 (2003).
23. Brown, L.A., Key, B.J. & Lovick, T.A. Inhibition of vasomotion in hippocampal cerebral arterioles during increases in neuronal activity. *Auton. Neurosci.* **95**, 137–140 (2002).
24. Langton, P.D., Nelson, M.T., Huang, Y. & Standen, N.B. Block of calcium-activated potassium channels in mammalian arterial myocytes by tetraethylammonium ions. *Am. J. Physiol.* **260**, H927–H934 (1991).
25. Silva, A.C., Lee, S.P., Iadecola, C. & Kim, S.G. Early temporal characteristics of cerebral blood flow and deoxyhemoglobin changes during somatosensory stimulation. *J. Cereb. Blood Flow Metab.* **20**, 201–206 (2000).
26. Silva, A.C., Lee, S.P., Yang, G., Iadecola, C. & Kim, S.G. Simultaneous blood oxygenation level-dependent and cerebral blood flow functional magnetic resonance imaging during forepaw stimulation in the rat. *J. Cereb. Blood Flow Metab.* **19**, 871–879 (1999).
27. Nagelhus, E.A. *et al.* Immunogold evidence suggests that coupling of K^+ siphoning and water transport in rat retinal Muller cells is mediated by a coenrichment of Kir4.1 and AQP4 in specific membrane domains. *Glia* **26**, 47–54 (1999).
28. Simard, M. & Nedergaard, M. The neurobiology of glia in the context of water and ion homeostasis. *Neuroscience* **129**, 877–896 (2004).
29. Wang, X. *et al.* Astrocytic Ca^{2+} signaling evoked by sensory stimulation *in vivo*. *Nat. Neurosci.* **9**, 816–823 (2006).
30. Simard, M., Arcuino, G., Takano, T., Liu, Q.S. & Nedergaard, M. Signaling at the gliovascular interface. *J. Neurosci.* **23**, 9254–9262 (2003).
31. Kuffler, S.W., Nicholls, J.G. & Orkand, R.K. Physiological properties of glial cells in the central nervous system of amphibia. *J. Neurophysiol.* **29**, 768–787 (1966).
32. Gebremedhin, D. *et al.* Metabotropic glutamate receptor activation enhances the activities of two types of Ca^{2+}-activated K^+ channels in rat hippocampal astrocytes. *J. Neurosci.* **23**, 1678–1687 (2003).
33. Meredith, A.L., Thorneloe, K.S., Werner, M.E., Nelson, M.T. & Aldrich, R.W. Overactive bladder and incontinence in the absence of the BK large conductance Ca^{2+}-activated K^+ channel. *J. Biol. Chem.* **279**, 36746–36752 (2004).
34. Newman, E.A. Regional specialization of retinal glial cell membrane. *Nature* **309**, 155–157 (1984).
35. Newman, E.A. High potassium conductance in astrocyte endfeet. *Science* **233**, 453–454 (1986).
36. Horiuchi, T., Dietrich, H.H., Tsugane, S. & Dacey, R.G., Jr. Role of potassium channels in regulation of brain arteriolar tone: comparison of cerebrum versus brain stem. *Stroke* **32**, 218–224 (2001).
37. Nelson, M.T. *et al.* Relaxation of arterial smooth muscle by calcium sparks. *Science* **270**, 633–637 (1995).
38. Iadecola, C. Neurovascular regulation in the normal brain and in Alzheimer's disease. *Nat. Rev. Neurosci.* **5**, 347–360 (2004).
39. Park, L. *et al.* Abeta-induced vascular oxidative stress and attenuation of functional hyperemia in mouse somatosensory cortex. *J. Cereb. Blood Flow Metab.* **24**, 334–342 (2004).
40. Cheney, J.A. *et al.* The maxi-K channel opener BMS-204352 attenuates regional cerebral edema and neurologic motor impairment after experimental brain injury. *J. Cereb. Blood Flow Metab.* **21**, 396–403 (2001).
41. Heurteaux, C., Bertaina, V., Widmann, C. & Lazdunski, M. K^+ channel openers prevent global ischemia-induced expression of c-fos, c-jun, heat shock protein, and amyloid beta-protein precursor genes and neuronal death in rat hippocampus. *Proc. Natl. Acad. Sci. USA* **90**, 9431–9435 (1993).
42. Jensen, B.S. BMS-204352: a potassium channel opener developed for the treatment of stroke. *CNS Drug Rev.* **8**, 353–360 (2002).
43. Gribkoff, V.K. *et al.* Targeting acute ischemic stroke with a calcium-sensitive opener of maxi-K potassium channels. *Nat. Med.* **7**, 471–477 (2001).
44. Cauli, B. *et al.* Cortical GABA interneurons in neurovascular coupling: relays for subcortical vasoactive pathways. *J. Neurosci.* **24**, 8940–8949 (2004).